Vital Annex: International Journal of Novel Research in Advanced Sciences
ISSN: 2751-756X
Volume 04 Number 06 (2025)
https://innosci.org/IJNRAS

Article

In Vitro Cytotoxicity Assessment of Green Synthesized CuO: NiO Nanocomposites Against Human Prostate Cancer Cells

Jawad N. K. Makassees[1], Ali K. Hattab[2], Ali A. Fayyadh[3]

1. Ministry of Education, General Directorate of Wasit Education, Wasit, Iraq.
2. Department of Physics, College of Science, University of Wasit, Wasit, Iraq.
3. Ministry of Education, General Directorate of Wasit Education, Wasit, Iraq.

* Correspondence: jalmaksusse@uowasit.edu.iq , ahatab@uowasit.edu.iq , alia224@uowasit.edu.iq

Abstract: In vitro cytotoxic evaluation of CuO:NiO nanocomposites synthesized using two phytogenic routes employing *Cinnamomum cassia* and *Mentha* plant extracts against human prostate cancer cell line (DU145) and human foreskin fibroblast (HFF) were investigated in this study. Also, comprehensive characterization to study the structural and morphological analyses using XRD, FTIR, FESEM, and EDX techniques. According to XRD, *Cinnamomum cassia*-mediated and *Mentha*-mediated nanocomposites formed crystalline phases with 25.14 nm and 20.27 nm crystallite sizes, respectively. FESEM observations revealed that the particles in *Cinnamomum cassia*-mediated nanocomposites are clustered and spherical, while in *Mentha*-mediated nanocomposites, they are more uniform in size and less likely to cluster. The elemental analysis of EDX found Cu, Ni, and O in both nanocomposites, but the *Cinnamomum cassia* had a higher amount of Cu (33.69%) and Ni (28.00%) than those prepared using *Mentha* (Cu: 21.87% and Ni: 22.10%). Both types of nanocomposites were found to have low toxicity toward the normal HFF cells, but were more selective cytotoxicity against the DU145 cancer cells. The anticancer effect of *Cinnamomum cassia*-based nanocomposites show greater (IC_{50} = 864.41 μg/mL) than that of *Mentha*-based nanocomposites (IC_{50} = 920.28 μg/mL). The morphological analysis of cells after cancer therapy showed that cell changes indicating apoptosis were more pronounced between 400-800 μg/mL. Based on the results, producing CuO:NiO nanocomposites with useful applications in cancer therapy can be achieved with green synthesis by using plant extracts, since the type of compounds in the extract greatly influences both the properties and the biological activity of the final nanocomposites.

Keywords: CuO:NiO nanocomposite, green synthesis, cytotoxicity, crystallite, prostate cancer.

Citation: Makassees, J. N. K, Hattab, A. K & Fayyadh, A. A. In Vitro Cytotoxicity Assessment of Green Synthesized Cuo: Nio Nanocomposites Against Human Prostate Cancer Cells. Vital Annex: International Journal of Novel Research in Advanced Sciences 2025, 4(6), 195-208.

Received: 10th Mar 2025
Revised: 16th Apr 2025
Accepted: 24th May 2025
Published: 23thJun 2025

1. Introduction

Nanotechnology has allowed for the development of new nanomaterials in medicine that safely and effectively treat cancer, while other treatments may not. Many researchers are attracted to metal oxide nanocomposites because they have high surface areas, several morphologies and strong catalytic activity [1,2]. Among nanostructures, copper oxide (CuO) and nickel oxide (NiO) are highly regarded in anticancer treatment because they kill cancerous cells with the help of reactive oxygen species (ROS), resulting in oxidative stress [1,3]. Generally, synthesising metal oxide nanoparticles involves hazardous materials and consumes a lot of energy which worries many people about the environment and safety for living organisms. Different from the previous method, green synthesis involving plant extracts is now preferred as a safe and eco-friendly choice, due to the reducing and stabilizing powers of plant-based chemicals [4,5]. The Phyto molecules not only decrease metal ions in the solution but also act as agents that cap the nanostructures and shape their appearance, size and stability in water [6]. Moreover, the bioactive compounds integrated within the plant extracts may

give the extracted nanocomposites extra biological properties, which may further promote the therapeutic effects of the extracts in a synergistic manner. The choice of the plant extracts has a great effect on the characteristics and activities of the nanoparticles. Plant extracts of *cinnamomum cassia* are rich in chemicals such as cinnamaldehyde, eugenol and polyphenols that have demonstrated some antimicrobial effects as well as anticancer and anti-free radical effects [7]. Such compounds contain functional groups which can reduce metal ions and stabilize nanoparticles by interacting with the surface. Likewise, Mentha plant extract is also a source of menthol, menthone, rosmarinic acid and flavonoids that possess various biological activities and can be successfully utilized in the production of nanoparticles [8]. Plant extracts play a major role in determining how the final nanoparticles will act physically and with biological materials. Bioactive chemicals including cinnamaldehyde, eugenol and different polyphenols with recognized antioxidant, antimicrobial and anticancer benefits are present in *Cinnamomum cassia* [9]. They are structured to react with metal ions reducing them and stabilize the surface of the nanoparticle through interactions. In addition, *Mentha* species are full of menthol, menthone, rosmarinic acid and flavonoids that have various biological activities and are useful for making nanoparticles [8]. Cancer nanotechnology is challenged by the need to selectively kill malignant cells without harming healthy ones. Because prostate cancer is the second most frequently diagnosed cancer in men [10], it should be a main focus in developing new treatment strategies. Since DU145 cells are from brain metastasis and act like androgen-independent prostate cancer, they are commonly used to study the efficacy of new anticancer substances in the laboratory. Metal oxide nanoparticles use a range of pathways to harm cells, including causing ROS, dysfunction of the mitochondria, changes in DNA and leaking of cell contents. cancer cells commonly react more strongly to agents that increase oxidative stress than healthy cells do. Having this differential susceptibility creates an opportunity for making cancer-selective medicines at the nanoscale [1]. Moreover, there is a special effect known as EPR in tumor tissues that allow nanoparticles to concentrate in those regions and in this way they become in a better position to target and destroy cancer cells [3]. Nevertheless, the application of metal oxide nanoparticles in clinics has been impeded with some key issues regarding toxicity, their localization in the body, and the rate of their clearance. Green synthesis is seen as a way to address these aspects and wants to reduce the use of harmful chemicals and use some milder, biological coating agents that have the potential to alter the way nanoparticles behave in live organisms. Also, there is a need to understand the impact of synthesis settings and plant chemicals on the properties of the nanoparticles to develop methods in which repetition can be achieved. This paper attempts to prepare CuO:NiO nanocomposites with *Cinnamomum cassia* and *Mentha* extracts and critically examine their characteristics through XRD, FTIR, FESEM and EDX. The study enables the capacity of these nanomedicines to kill prostate cancer cells (DU145) in the lab relative to normal cells (HFF). This study helps advance the development of metal oxide nanocomposites in cancer treatment by understanding the relationships among how they are produced, what they look like and their activities in the body.

2. Materials and Methods

2.1. Materials

Copper (II) nitrate trihydrate (Cu $(NO_3)_2 \cdot 3H_2O$, 99.5%) and "nickel (II) nitrate hexahydrate ($Ni(NO_3)_2 \cdot 6H_2O$, 98%)" were the metals used in the making of CuO:NiO nanocomposites. *Cinnamomum cassia* bark and fresh *Mentha* leaves were all thoroughly cleaned in deionized water, air-dried at room temperature for three days, minced to fine particles and transferred to airtight containers at 4°C until used. Use RPMI-1640 medium with 10% fetal bovine serum (FBS), 1% penicillin-streptomycin solution, 0.25% trypsin-EDTA solution, sterile phosphate-buffered saline (PBS, pH 7.4), human prostate cancer cell line (DU145) and human foreskin fibroblast (HFF) obtained from American Type Culture Collection (ATCC, Manassas, VA, USA), 3-(4,5-dimethyl).

2.2. Methods

2.2.1. Cell culture

Cells from the human prostate cancer cell line (DU145) and human foreskin fibroblast (HFF) were obtained from the American Type Culture Collection (ATCC, Manassas, VA, USA). RPMI-1640 medium combined with 10% fetal bovine serum (FBS) and 1% penicillin-streptomycin solution served as the growth medium for cells during culture. The cultures received incubation at 37°C under atmospheric conditions with 5% CO_2 levels along with high humidity. The subculture occurred whenever cells achieved 80-85% confluence by using a trypsin-EDTA solution at 0.25%.

2.2.2. Preparation of nanocomposite suspensions

Nanocomposite samples of CuO: NiO were dispersed in sterile phosphate-buffered saline (PBS, pH 7.4) for 15 minutes while using sonication at a pulse mode with 5 s of operation followed by 3 s intervals to achieve uniform dispersion. Culture medium served to dilute stock suspensions until concentrations reached 25, 50, 100, 200, 400, and 800 μg/mL for cytotoxicity testing.

2.2.3. MTT assay

Cell viability measurement occurred through MTT assay. The cells developed from DU145 and HFF were seeded at 1×10^4 cells/well density within 96-well plates before allowing 24-hour adherence.

The cell incubation duration at 48 h utilized fresh medium containing different copper oxide nanocomposite concentrations from 25 to 800 μg/mL. The MTT solution (5 mg/mL in PBS) at 20 μL volume was added to each well before a 4- hour incubation at 37°C. The analyzed wavelength for measuring formazan crystallite absorbance corresponded to 570 nm through a BioTek Instruments microplate reader (operations in Winooski, VT, USA) with 630 nm as its reference wavelength. The formazan crystals were solubilized using 100 μL DMSO. The cell viability is given by the formula:

$$Cell\ viability = \left(\frac{Absorbance\ of\ treated\ cells}{Absorbance\ of\ control\ cells}\right) \times 100\ \% \ldots\ldots\ldots\ldots\ldots\ldots 1$$

The half-maximal inhibitory concentration (IC_{50}) values emerged through GraphPad Prism (software version 8.0, GraphPad Software, San Diego, CA, USA) from dose-response curve graphs.

Morphological Analysis

A 48-hour exposure to various concentrations of nanocomposites made the microscopic changes in the cells visible under phase-contrast microscopy. Sample photographs were also recorded by the study team to assess the response of various doses of drugs on cell structural appearance and cell population density.

2.2.4. Characterization Techniques

CuO:NiO nanocomposites have been studied in a proper manner by multiple advanced analytical techniques. The structure was analyzed with a D8 advance X-ray diffractometer (Bruker) and monochromated Cu Kalpha radiation (1.5406 A^0) at 50 kV and 40 mA. The X-ray diffractometer gathered the diffraction data at the ranges of 20^0 to 90^0 degrees with a 0.01 degree step length and a 1.5 s time-per-step which enabled the accurate crystallite phase identification and crystal sizes measurement through the Scherrer equation. Chemical bonding and functional group analysis was carried out on an FT-IR spectra collection process accomplished by a Jasco FT/IR-4600 spectrometer equipped with a DLATGS detector. Measurement in the mid-IR region (4000400 cm^{-1}) allowed direct analysis of the powder through the use of the DRIFTS sampling technique. The spectra that were observed revealed successful formation of metal oxide, having discrete peaks that were indicative of both Cu–O and Ni–O stretching vibrations. Imaging was done using an FESEM-type Hitachi SU8220 at accelerating voltage of 20 kV.The tool enabled the users to study surface characteristics along with the distribution patterns of nanoparticles and sizes at a high magnification. Further elemental analysis was performed in collaboration with the assistance of EDS detector which had been invented by EDAX. The quantitative energy-dispersive X-ray spectroscopy (EDX) laboratory data were used to establish the presence of Cu, Ni, and O elements and provided stoichiometric and uniform data on the synthesized CuO:NiO nanocomposites.

3. Results and Discussion

Investigations of the crystal structures that formed during the synthesis of the CuO:NiO nanocomposite were provided by X-ray diffraction (XRD) analysis. X-ray diffraction works on the principle of Bragg law which forms a relationship between the interplanar spacing and the diffraction angle.

$$n\lambda = 2d\ \sin\theta \ldots\ldots\ldots\ldots\ldots 2$$

The X-ray diffraction pattern relies on four key factors that comprise the diffraction order (n) and X-ray wavelength (λ) and also crystal lattice plane distance (d) and X-ray beam incident angle (θ). This relation is a building block in the discovery of crystal structure in crystalline substances [11]. The crystallites size (D) was measured by use of the Scherrer equation.

$$D = (k\lambda)/(\beta \cos\theta) \ldots\ldots\ldots\ldots\ldots 3$$

The XRD peak analysis depends on K as the shape factor having a value of 0.94 and λ / 0.154060 nm as the wavelength of the CuKα radiation and β as the full width at half maximum (FWHM) as a measure of the width of the peak in radians and 0 as the Bragg diffraction angle [12]. The XRD patterns in Figs. 1 and 2 display distinct peaks attributed to monoclinic CuO (COD entry: 96-901-5823/96-901-6106) together with cubic NiO (COD entry: 96-432-0506) phases. For both *Cinnamomum*-mediated and *Mentha*-mediated samples the strongest XRD peaks appeared at 36.87°, 38.54° and 43.00° and at 37.03°, 38.70° and 43.01° respectively. The (111) and (200) crystal plane peaks alongside peak (111) indicate that pure crystalline nanocomposite substances have formed without detectable impurity phases. Standard d-spacing values demonstrate close correspondence to experimental measurements while minor deviations may stem from both lattice strain and size effects caused by the biomolecules occurring in plant extracts [13].

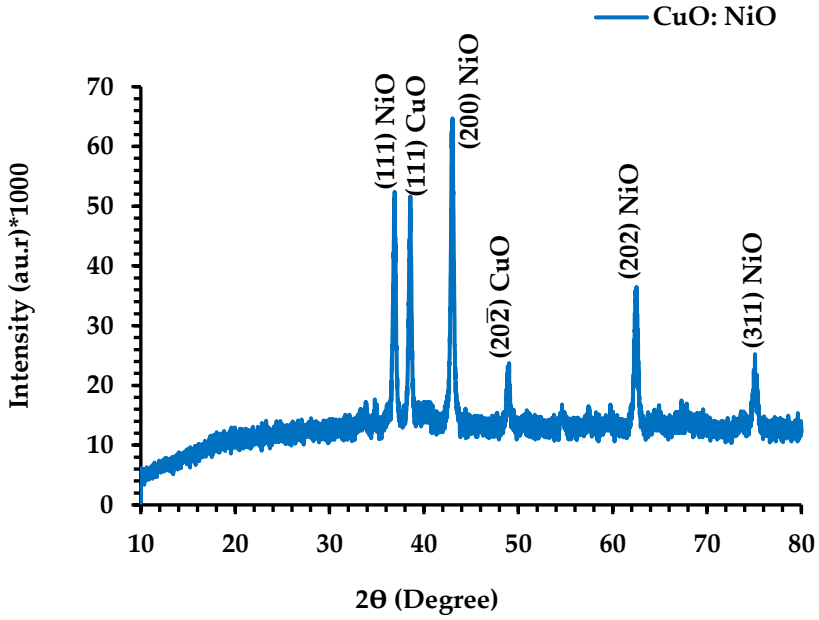

Figure 1. XRD pattern of *Cinnamomum cassia*-mediated CuO:NiO nanocomposite.

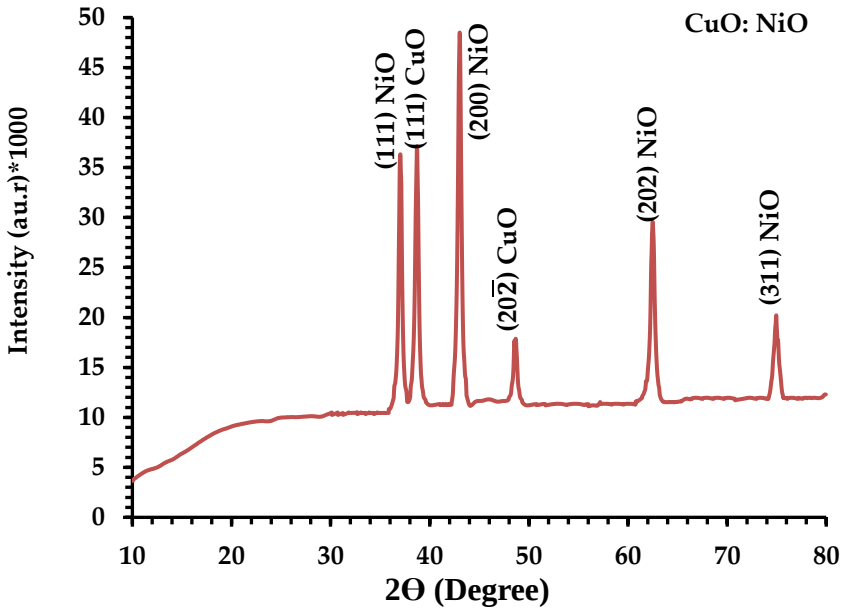

Figure 2. XRD pattern of *Mentha*-mediated CuO:NiO nanocomposite.

The d-spacings of the *Cinnamomum*-mediated sample showed experimental measurements at 2.4349 Å, 2.3339 Å, and 2.1018 Å that closely matched standard values at 2.4251 Å, 2.3392 Å, and 2.1005 Å. The *Mentha*-mediated sample obtained d-spacing values at 2.4257 Å, 2.3240 Å and 2.1014 Å which matched closely with the standard values of 2.4254 Å, 2.3207 Å and 2.1003 Å. The crystallite sizes determined by Scherrer equation analysis indicated substantial differences in the production methods. *Cinnamomum cassia*-mediated nanocomposite synthesized larger crystallite dimensions (25.14 nm) than *Mentha*-mediated nanocomposite with dimensions (20.27 nm). Analysis shows that different growth mechanisms controlled by plant extract phytochemical formulations influence the crystallite size variations [14]. The *Cinnamomum cassia* -mediated sample formed crystallites measuring 25.75, 25.84, and 23.82 nanometers in size for its three principal peaks and the crystallites of the *Mentha*-mediated sample reduced to 20.99, 20.48, and 19.33 nanometers. The crystallite sizes decreased in the *Mentha*-mediated sample because its high polyphenols and flavonoids content effectively limited nanoparticle growth at nucleation and crystallization stages [5]. The analysis of the nanocomposites demonstrates that plant extract selection directly affects crystallographic properties in the final structures. The *Mentha* extract demonstrates superior capping properties such that crystallite sizes remain smaller and surface area-to-volume ratios become higher. Surface reactivity functions as a key factor in catalytic processes and sensing applications and this characteristic turns out beneficial due to its presence [15]. Both samples show identical d-spacing patterns between their experimental and standard data thus revealing stoichiometric formation of CuO and NiO crystal phases with small lattice deformation even though synthesis methods were different. The slight peak position and intensity variations indicate that defect concentration and strain differences along with crystallinity changes result from the specific biomolecules within each plant extract [16]. The FTIR spectrum of *Cinnamomum cassia*-mediated CuO nanocomposite (Fig. 3) displays numerous distinctive absorption bands which reveal information about its molecular framework and surface modifications. The primary spectral bands of this spectrum are simultaneously produced by both oxide material of the metal and organic compounds of the plant extract materials. Presence of hydroxyl group along with water molecules attached to surfaces of nanoparticles are evidenced by the O-H stretching vibrations that form a broad absorption band between 3200-3600 cm^{-1} [17]. Absorption bands between 2850-2950 cm^{-1} indicate C-H stretching from methyl and methylene groups which exist within the organic *Cinnamomum cassia* compounds especially cinnamaldehyde and eugenol [18].

The absorption bands between 1600-1700 cm^{-1} detect C=O stretching vibrations from carbonyl compounds like aldehydes and ketones and the peaks within 1450-1650 cm^{-1} signify C=C stretching vibrations of aromatic rings [18]. The appearance of bands through spectrum analysis confirms how polyphenolic compounds from the *Cinnamomum cassia* extract bind onto surface areas of nanoparticles. The fingerprint region (1400-400 cm^{-1}) reveals metal-oxygen vibrational modes that produce bands between 500-700 cm^{-1} which correspond to Cu-O and Ni-O stretchings. The formation of CuO and NiO crystalline phases becomes validated by the appearance of these bands [19].

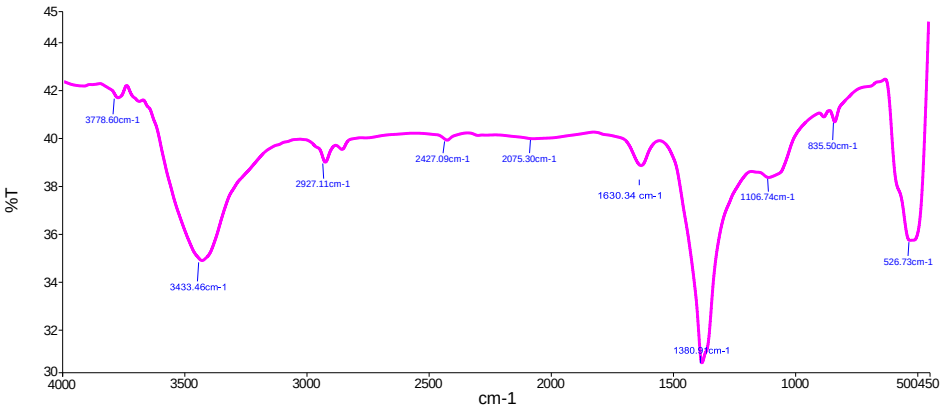

Figure 3. FTIR pattern of *Cinnamomum cassia*-mediated CuO:NiO nanocomposite.

The interaction between plant-derived organic compounds and metal oxide surface is confirmed through the appearance of C-O stretching vibrations between 1000-1100 cm^{-1} [20]. The FTIR spectrum of *Mentha*-CuO nanocomposites displays different absorption patterns than *Cinnamomum* cassia-CuO nanocomposites which indicates the distinct phytochemical features of *Mentha*-based extract in Fig. 4. Hydroxyl groups show their appearance as a broad band between 3200-3600 cm^{-1} in the FTIR spectrum just like the *Cinnamomum cassia*-mediated sample. The intensity together with breadth of this band differs from the others demonstrating various degrees of hydroxylation and hydrogen bonding occurrence as reported in [21]. The C-H stretching vibrations at 2850-2950 cm^{-1} present different intensity levels in the *mentha* extract compared to those of the *Cinnamomum cassia*-mediated control sample which demonstrates their unique aliphatic content composition [7].

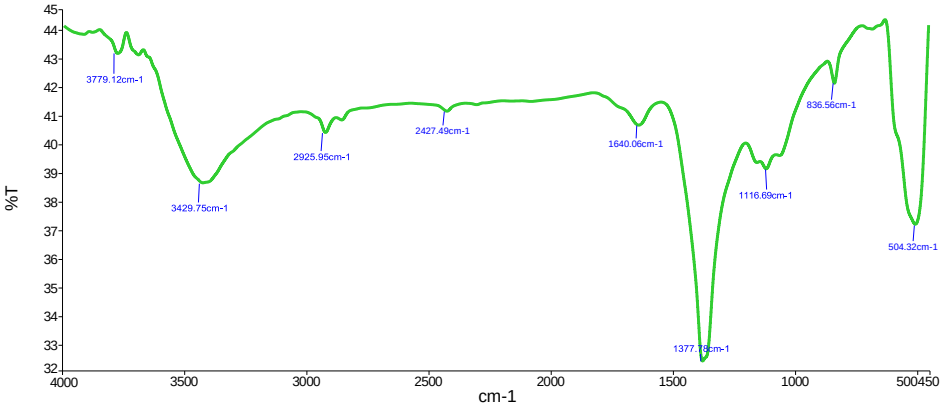

Figure 4. FTIR pattern of *Mentha*-mediated CuO:NiO nanocomposite.

The carbonyl stretching region (1600-1700 cm^{-1}) contains bands that help identify the functional groups of menthol and menthone and other terpenoids which exist in *Mentha* extract [22]. The 1400-1600 cm^{-1} absorption bands originate from aromatic C=C stretching vibrations as well as from C-H bending vibrations of methyl groups. Both CuO and NiO crystalline phases form as indicated by metal-oxygen vibrational modes in the fingerprint region between 500-700 cm^{-1}. The *Cinnamomum cassia*-mediated spectral bands exhibit stronger intensities and modify peak positions which indicates differences in the crystalline nature and particle size dimensions as well as possible changes in Cu ratio [23].

Identical functional groups detected in both samples indicate that phytochemicals including polyphenols and flavonoids as well as other phytochemicals participate in metal ion reduction and nanoparticle encapsulation. The peak diversity in intensity together with placement and form indicates dissimilar molecular interactions which result in various binding mechanisms. In the aromatic compounds and carbonyl groups spectral regions, there are strong absorption bands due to the presence of cinnamaldehyde and eugenol in high quantities in cinnamon extract. The hydroxyl and carbonyl functional groups are used to reduce their potential metal ion reducing compounds [4]. Spectral characteristics of Mentha-mediated sample contain characteristic features that confirm the occurrence of menthol and menthone as well as monoterpenoids. The nanocomposite includes compounds having various functional groups that may bind metal ions in various coordination modes hence influencing crystal formation and surface properties [24]. The FESEM images demonstrate the evident differences in the structure of the both CuO:NiO nanocomposites produced through green synthesis. Fig. 5. FESEM images of (a-left) Cinnamomum cassia-mediated nanocomposite are predominantly of a spherical structure and can be seen to be forming into agglomeration. The particles prefer to form groups and these groups possess disproportional edges and various sizes. This trend is in line with other works that have been published that attribute the mediating activity of cinnamaldehyde and eugenol in the development of metal oxide nanoparticles to cinnamon. However, Fig. 5. The Mentha- mediated CuO:NiO nanocomposite in (a- left) FESEM images depict reduced agglomeration and even smaller distribution of particle sizes. Individual nanostructures have been separated and well spaced by spraying.

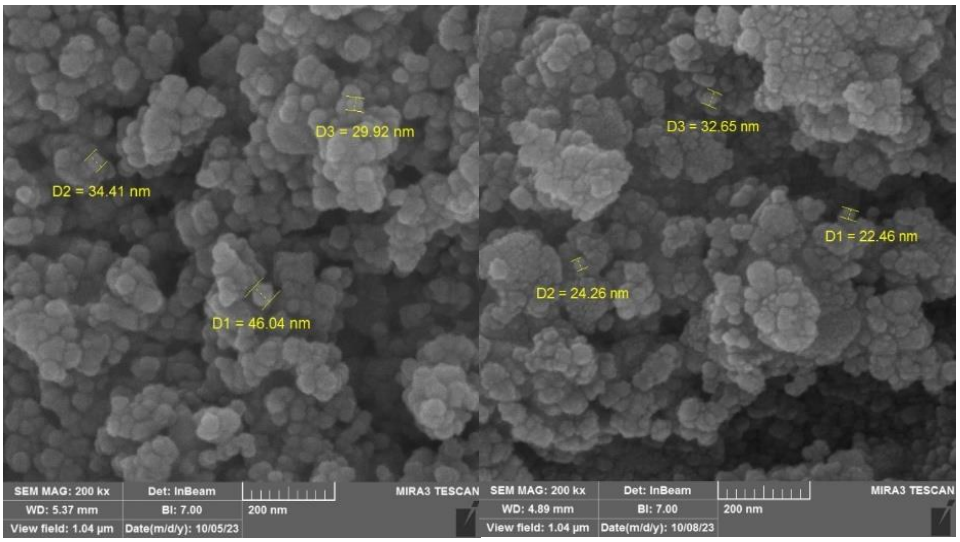

Figure 5. FESEM images of (a-left) *Cinnamomum cassia*-mediated CuO:NiO and (b-right) *Mentha*- mediated CuO:NiO nanocomposites.

The enhanced dispersion is attributed to the high capping effect of menthol and flavonoids found in Mentula which stabilize the nanoparticles and enable them to resist the extensive aggregation during formation and growth. Based on the FESEM pictures and XRD analysis, we see that the crystallite size of *Mentha*-mediated nanocomposites (20.27 nm) is smaller compared to that of the formed by using *Cinnamomum cassia* (25.14 nm). *Mentha* enhances better dispersion of particles reducing their size, so we obtain improved samples of good surface- to- volume ratios. This may be applicable in both catalysis activity and in biology. Nanoparticle morphology matters as it determines how nanoparticles enter the cells, where they localize in the body and the effectiveness of their treatment functions. While the lower agglomeration in *Mentha*-mediated samples indicates they might reach cells more easily, *Cinnamomum cassia*-mediated samples kill cancer cells more effectively, suggesting other factors are at work. EDX spectrum shown in fig. 6. confirmed the presence of all the elements in both nanomaterials and confirmed that the synthesis of CuO:NiO mixtures was successful.

The expected elements found in the *Cinnamomum cassia*-mediated nanocomposite are Cu, Ni and O, with measurements giving Cu (33.69%), Ni (28.00%) and O (35.30%) and some carbon content (3.01%) likely left by plant extract residues [25]. The near 1.2:1 Cu:Ni ratio means that these nanocomposites contain a little more copper than nickel [26].

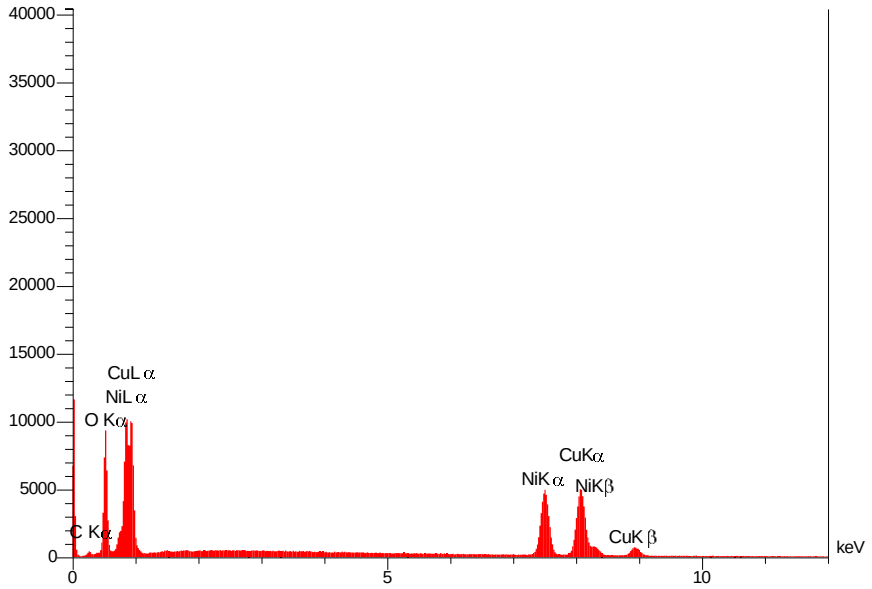

Figure 6. EDX spectrum of *Cinnamomum cassia*-mediated CuO:NiO nanocomposite.

In the EDX spectrum of the *Mentha*-mediated CuO:NiO nanocomposite shown in fig. 6, the element rates are different, with Cu at 21.87%, Ni at 22.10% and O at 34.04%, meaning there is a near-equal amount of Cu and Ni [27]. In addition, it should be noted that this sample carries 16.13% sodium and 3.15% nitrogen, whereas *Cinnamomum cassia*-based samples lack these elements completely. Sodium in the *Mentha*-mediated sample could result from the way *Mentha* extracts and synthesis differ compared to the control [28], [29].

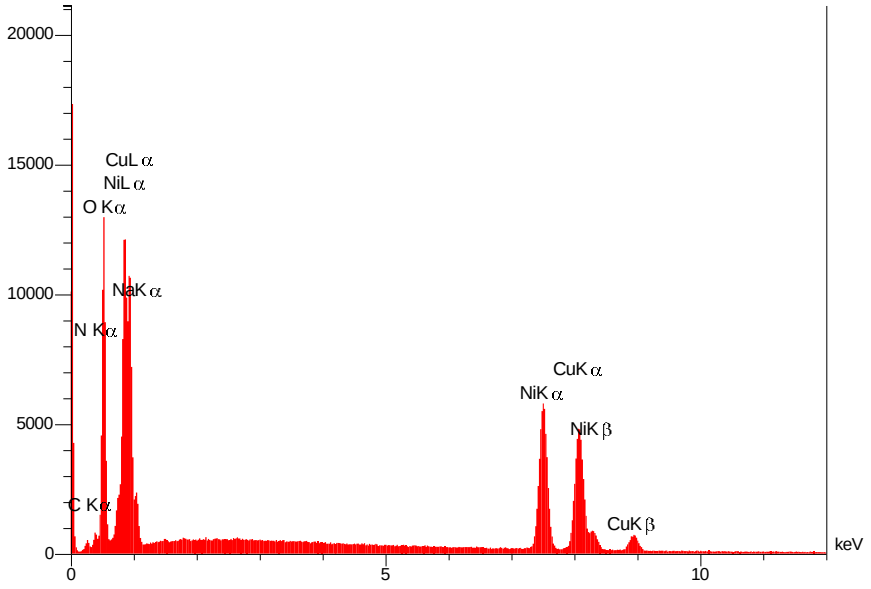

Figure 7. EDX spectrum of *Mentha*-mediated CuO:NiO nanocomposite.

Because both nanocomposites differ greatly in their compositions of elements, their physicochemical features and activities towards cells are influenced mainly by this difference [30]. A greater balance of Cu:Ni in the *Mentha*-mediated sample suggests the same amount of each metal oxide was incorporated uniformly, while the extra metals present in the *Cinnamomum cassia*-mediated sample may give it a slightly higher ability to damage cancer cells [31]. The presence of 35.30% oxygen in *Cinnamomum cassia*-mediated nanocomposites and 34.04% in *Mentha*-mediated ones confirms that metal oxide phases were formed successfully. XRD confirmed that there is CuO and NiO in the final structure, so the presence of oxygen in the sample shows that the process correctly produced these crystalline phases. The presence of oxygen affects both the characteristics and the biological actions of the nanocomposites, since the metal bonds with oxygen help cause oxidative stress to cancer cells. Comparing elemental composition with biological activities revealed that *Cinnamomum cassia*-synthesized nanocomposites had a slightly higher anticancer effect than *Mentha*-synthesized ones. The presence of more metal oxide can promote the production of reactive oxygen species which is thought to lead to cancer cell death.

As presented in Table 1. DU145 cells exhibited concentration-dependent toxicity against both nanocomposites but remained minimally toxic to normal HFF cells. *Cinnamomum cassia*-mediated CuO:NiO nanocomposite demonstrated a decreased viability effect as cells progressed from 100.065±3.862% at 25 μg/mL to 60.273±13.047% at 800 μg/mL. The nanocomposites derived from *Mentha* also demonstrated a reduction in DU145 cell viability levels which started at 87.711±11.5% with 25 μg/mL and ended at 58.842±20.483% with 800 μg/mL. The viability levels of normal HFF cells demonstrated significant elevation throughout all tested concentrations. The viability of HFF cells ranged between 103.882±25.592% at 25 μg/mL and 77.242±9.178% at 800 μg/mL in testing *Cinnamomum cassia*-mediated nanocomposites. Effective HFF viability remained between 101.758±25.966% and 82.417±2.753% throughout the entire concentration range of *Mentha*-mediated nanocomposites.

Table 1. Cytotoxicity effect of *Cinnamomum cassia*-mediated and *Mentha*-mediated - CuO:NiO nanocomposites on DU145 and HFF cells after 48 hours of incubation at 37ºC.

Concentration μg mL^{-1}	**Mean Viability (%) ± SD**			
	Cinnamomum cassia-mediated CuO:NiO nanocomposite		*Mentha*-mediated CuO:NiO nanocomposite	
	DU145	HFF	DU145	HFF
800	60.273 ± 13.047	77.242 ± 9.178	58.842 ± 20.483	82.417 ± 2.753
400	60.013 ± 7.410	79.413 ± 19.373	59.492 ± 25.591	86.007 ± 5.446
200	61.508 ± 20.410	83.222 ± 6.218	71.301 ± 9.556	89.230 ± 3.109
100	61.248 ± 11.030	82.564 ± 10.531	76.723 ± 12.355	88.351 ± 6.658
50	91.937 ± 18.357	85.201 ± 6.396	82.509 ± 4.645	91.648 ± 5.560
25	100.065± 3.862	103.882±25.592	87.711± 11.5	101.758±25.966

The cytotoxic behavior of *Cinnamomum cassia*-mediated and *Mentha*-mediated CuO:NiO nanocomposites varies across Figs. 8 and 9 regarding their influence on the cell lines. The microscopic analysis of cell death using dose-response curves determined the IC_{50} value for *Cinnamomum cassia*-mediated to be 864.41 µg/mL while the IC_{50} value for *Mentha*- mediated nanocomposites became 920.28 µg/mL against DU145 cells thus showing a slight advantage in anticancer activity for the *Cinnamomum cassia*-mediated formulation.

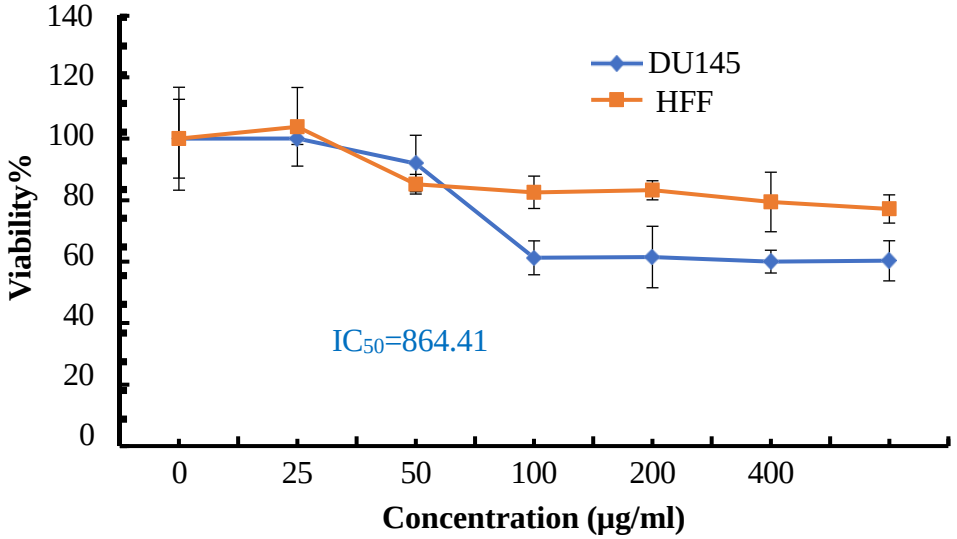

Figure 8. Cytotoxic effect of *Cinnamomum cassia*-mediated -CuO:NiO nanocomposite on DU145 and HFF cells after 48 hrs incubation at 37 ºC.

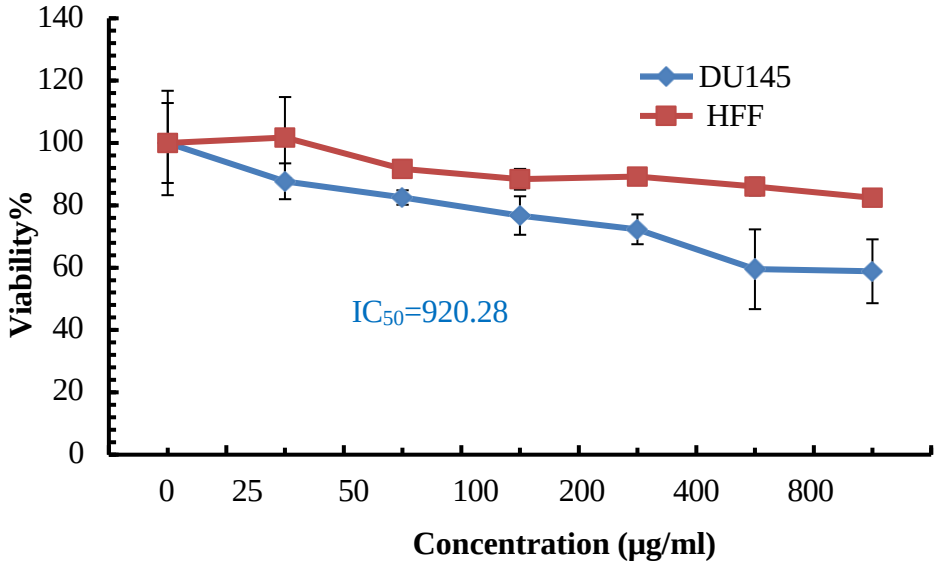

Figure 9. Cytotoxic effect of *Mentha*-mediated - CuO:NiO nanocomposite on DU145 and HFF cells after 48 hrs incubation at 37 ºC.

The DU145 cellular morphological alterations caused by *Cinnamomum cassia*-mediated and *Mentha*-mediated CuO:NiO nanocomposites at different concentrations appear in Fig. 10.

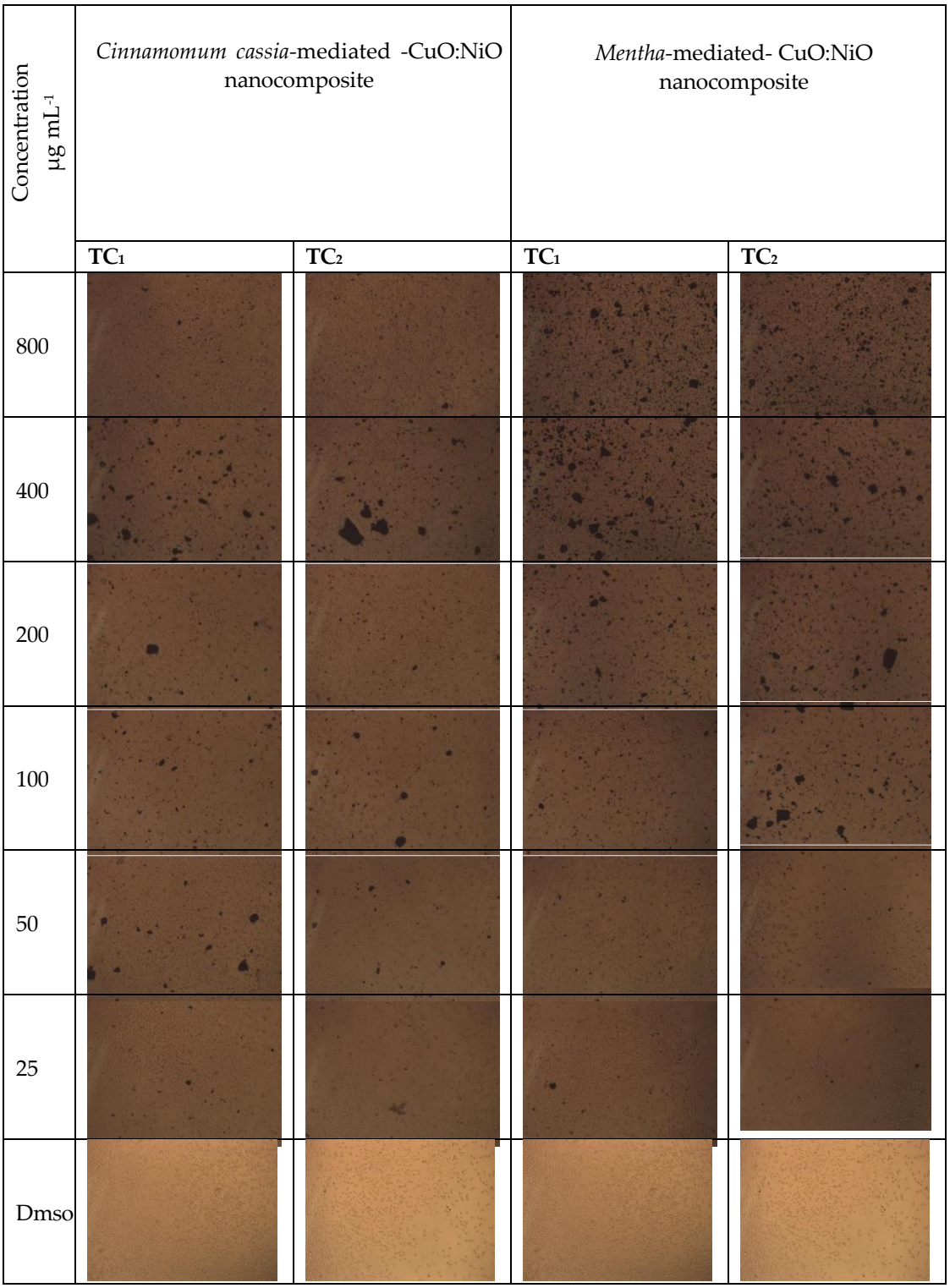

Figure 10. Dose-response curve of DU145 prostate cancer cells treated with *Cinnamomum cassia*-mediated - *Mentha*-mediated CuO:NiO nanocomposites as determined by MTT assay.

The results presented through the TC_1 and TC_2 columns demonstrate the repeated testing of each concentration while showing the consistency of the obtained results. The cells showed minimal morphological modifications while being treated with *Cinnamomum cassia* concentrations between 25-50 μg/mL than when compared to DMSO controls. At 100-800 μg/mL the cells displayed a sequence of morphological changes resulting in cell contraction together with membrane abnormality reduced cell numbers and absence of epithelial characteristics. Data showed larger cell alterations in *Cinnamomum cassia*-mediated nanocomposites-treated cells than cells given *Mentha*-mediated nanocomposites at identical concentrations during the time period 400-800 μg/mL (Fig. 10) in accordance with the quantitative viability measures in Table 1. The results were confirmed through combined numerical viability measurements (Table 1) as well as visual inspections (Fig. 10). The selective destruction of cancer cells over normal cells serves as a significant benefit for potential anticancer uses since it deals with the main weakness of standard chemotherapeutic treatments [32]. Multiple factors explain why cancer cells remain more sensitive to cytotoxicity than normal cells during nanoparticle treatments. Nanoparticles cause oxidative stress that impacts cancer cells over normal cells due to the fact that the cancer cells sustain altered metabolism that involves higher reactive oxygen species and lower antioxidant defenses [33]. Better nanoparticle concentration potential is associated with the enhanced permeability and retention (EPR) effect [34]. Cytotoxicity assays indicate that the nanocomposite of *Cinnamomum cassia* extract (IC50 = 864.41 μg/mL) has a little higher potential of interacting with DU145 cells compared to another nanocomposite prepared using *Mentha* extract (IC_{50} = 920.28 μg/mL). This means that plant extracts have phytochemical components that can either effectively alter the biological activities of the resulting nanocomposite products. *Cinnamomum cassia* contains bioactive constituents containing cinnamaldehyde and polyphenols along with eugenol that have cell-destroying activity alone and enhance the toxicity of metal oxide nanocomposites. According to [8]. The biological activity of nanocomposite obtained by Mentha species will be influenced by various substances such as menthol, rosmarinic acid, flavonoids, among others Cytologic studies of DU145 cell lines subjected to nanocomposites identified the changes equivalent to previously reported apoptotic profiles in the literature on metal oxide nanoparticle (Fig. 10). Patterns that are known to happen in normal apoptosis were preserved by the shrinkage of cells in our experiments and their alteration in density [33]. Despite the targeted anticancer effects, these nanocomposites require augmentation to produce better therapeutic effects as the IC_{50} ranges are higher than 800 0g/mL. The therapeutic properties of such nanocomposites can be enhanced by the modern state of work on the principles of nanoparticle functionalization of the surface layer and controlled release and targeted delivery systems. Once the nanocomposites combine with traditional chemotherapeutic agents the effects will be synergistic resulting in less dosage being needed and potential toxicity is also minimized [10]. The cytotoxicity of DU145 cells towards both nanocomposites had a dose-dependent response but the *Cinnamomum cassia*-mediated nanocomposites were observed to have remained resistant to alteration in cell viability at 100-800 μg/mL concentrations (Table 1). The plateau effect on cellular uptake and adaptation effects observed highlights the importance of studying nanoparticles-cell interaction at different concentrations.

4. Conclusion

This step-by-step analysis shows that the selection of the plant extract has a significant impact on the chemical and biological characteristics of the nanocomposites of CuO:NiO. The observation of FESEM indicated that *Cinnamomum cassia*-tissue nanocomposites were surface different, whereas *Mentha*-tissue composite particles were more homogenous and did not agglomerate strongly because Mentha phytochemicals coated them efficiently. The EDX analysis showed that both of the methods formed CuO:NiO nanocomposites with predicted ratios of the elements, however, the concentration of the elements Cu and Ni was slightly different in the products. Correlations were found between the atomic and microscopic properties of these compounds and their observed actions against prostate cancer cells.

The results revealed that both nanocomposites harmed cancer cells but were nearly harmless to normal HFF cells, making them promising for targeted treatments. It is believed that both cinnamaldehyde and eugenol present in *Cinnamomum cassia* contribute to its slightly better anticancer performance compared to *Mentha*-mediated nanocomposites. Observed changes in form following treatment demonstrate that apoptosis is the main way the cells die. Although selective cytotoxicity has been seen, the low potency calls for improving the effectiveness before further development. Further studies on how to surface-modify, add targeting molecules and complement current anticancer medicines may make these therapies more powerful and still selective. Findings could be applied to health care if researchers study the molecular causes and conduct in vivo experiments. It is found that green synthesis can be used to develop CuO:NiO nanocomposites with potential cancer nanomedicine uses, highlighting the key role of plant-based compounds in shaping nanoparticle qualities and the effects on cancer therapy.

REFERENCES

[1] Abdal Dayem, M. K. Hossain, S. Bin Lee, K. Kim, S. K. Saha, G.-M. Yang, et al., "The role of reactive oxygen species (ROS) in the biological activities of metallic nanoparticles," Int. J. Mol. Sci., vol. 18, p. 120, 2017.

[2] P. Khanna, C. Ong, B. H. Bay, and G. H. Baeg, "Nanotoxicity: an interplay of oxidative stress, inflammation and cell death," Nanomaterials, vol. 5, pp. 1163–1180, 2015.

[3] J. K. Patra, G. Das, L. F. Fraceto, E. V. R. Campos, M. del P. Rodriguez-Torres, L. S. Acosta-Torres, et al., "Nano based drug delivery systems: recent developments and future prospects," J. Nanobiotechnol., vol. 16, pp. 1–33, 2018.

[4] A. M. El Shafey, "Green synthesis of metal and metal oxide nanoparticles from plant leaf extracts and their applications: A review," Green Process. Synth., vol. 9, pp. 304–339, 2020.

[5] M. Pirsaheb, T. Gholami, H. Seifi, E. A. Dawi, E. A. Said, A.-H. M. Hamoody, et al., "Green synthesis of nanomaterials by using plant extracts as reducing and capping agents," Environ. Sci. Pollut. Res., vol. 31, pp. 24768–24787, 2024.

[6] A. K. Mittal, Y. Chisti, and U. C. Banerjee, "Synthesis of metallic nanoparticles using plant extracts," Biotechnol. Adv., vol. 31, pp. 346–356, 2013.

[7] C. Zhang, L. Fan, S. Fan, J. Wang, T. Luo, Y. Tang, et al., "Cinnamomum cassia Presl: A review of its traditional uses, phytochemistry, pharmacology and toxicology," Molecules, vol. 24, p. 3473, 2019.

[8] F. Brahmi, M. Khodir, C. Mohamed, and D. Pierre, "Chemical composition and biological activities of Mentha species," in Aromatic and Medicinal Plants - Back to Nature, IntechOpen, 2017.

[9] D. Zhang, C. Jin, H. Tian, Y. Xiong, H. Zhang, P. Qiao, et al., "An in situ TEM study of the surface oxidation of palladium nanocrystals assisted by electron irradiation," Nanoscale, vol. 9, pp. 6327–6333, 2017.

[10] A. Prasad, M. M. Bakr, and A. N. ElMeshad, "Surface-functionalised polymeric nanoparticles for breast cancer treatment: Processes and advances," J. Drug Target., vol. 32, pp. 770–784, 2024.

[11] B. D. Cullity and R. Smoluchowski, "Elements of X-ray Diffraction," Phys. Today, vol. 10, p. 50, 1957.

[12] A. Monshi, M. R. Foroughi, and M. R. Monshi, "Modified Scherrer equation to estimate more accurately nano-crystallite size using XRD," World J. Nano Sci. Eng., vol. 2, pp. 154–160, 2012.

[13] V. Selvanathan, M. Shahinuzzaman, S. Selvanathan, D. K. Sarkar, N. Algethami, H. I. Alkhammash, et al., "Phytochemical-assisted green synthesis of nickel oxide nanoparticles," Catalysts, vol. 11, p. 1523, 2021.

[14] R. Sharma, A. Dhillon, and D. Kumar, "Mentha-stabilized silver nanoparticles for high-performance colorimetric detection of Al (III)," Sci. Rep., vol. 8, p. 5189, 2018.

[15] R. Dash and A. S. Bhattacharyya, "Sequential growth mechanism of Ni-doped CuO nanocrystallites," MRS Adv., vol. 8, pp. 937–942, 2023.

[16] R. López González, M. H. Gutiérrez, R. L. García, S. A. Gómez Cornelio, C. Lobato, A. Gómez-Rivera, et al., "ZnO nanomaterials with enhanced antimicrobial activity," J. Chem. Technol. Biotechnol., vol. 99, pp. 2535–2544, 2024.

[17] Y. Li, D. Kong, and H. Wu, "Analysis and evaluation of essential oil components of cinnamon barks using GC–MS and FTIR spectroscopy," Ind. Crops Prod., vol. 41, pp. 269–278, 2013.

[18] I. Z. Luna, L. N. Hilary, A. M. S. Chowdhury, M. A. Gafur, N. Khan, and R. A. Khan, "Preparation and characterization of copper oxide nanoparticles synthesized via chemical precipitation method," Open Access Libr. J., vol. 2, pp. 1–8, 2015.

[19] Y. Huang, Y. Liu, H. Tan, Y. Cheng, K. Tao, D. Gu, et al., "Assessing essential oil composition in Cinnamomum cassia leaves using GC-MS and FTIR," Czech J. Food Sci., vol. 42, 2024.
[20] M. Alavi, S. Dehestaniathar, S. Mohammadi, A. Maleki, and N. Karimi, "Antibacterial activities of phytofabricated ZnO and CuO NPs," Adv. Pharm. Bull., vol. 11, pp. 497–505, 2020.
[21] O. Taylan, N. Cebi, and O. Sagdic, "Rapid screening of Mentha spicata essential oil and L-menthol in Mentha piperita oil," Foods, vol. 10, p. 202, 2021.
[22] V. V. Makarov, A. J. Love, O. V. Sinitsyna, S. S. Makarova, I. V. Yaminsky, M. E. Taliansky, et al., "Green nanotechnologies: synthesis of metal nanoparticles using plants," Acta Naturae, vol. 6, pp. 35–44, 2014.
[23] A. K. Mittal, Y. Chisti, and U. C. Banerjee, "Synthesis of metallic nanoparticles using plant extracts," Biotechnol. Adv., vol. 31, pp. 346–356, 2013.
[24] J. K. Patra, G. Das, L. F. Fraceto, E. V. R. Campos, M. del P. Rodriguez-Torres, L. S. Acosta-Torres, et al., "Nano based drug delivery systems: recent developments and future prospects," J. Nanobiotechnol., vol. 16, pp. 1–33, 2018.
[25] A. M. El Shafey, "Green synthesis of metal and metal oxide nanoparticles from plant leaf extracts," Green Process. Synth., vol. 9, pp. 304–339, 2020.
[26] F. Brahmi, M. Khodir, C. Mohamed, and D. Pierre, "Biological activities of Mentha species," in Aromatic and Medicinal Plants, IntechOpen, 2017.
[27] Y. Huang, Y. Liu, H. Tan, Y. Cheng, K. Tao, D. Gu, et al., "Essential oil composition in Cinnamomum cassia leaves," Czech J. Food Sci., vol. 42, 2024.
[28] D. Zhang, C. Jin, H. Tian, Y. Xiong, H. Zhang, P. Qiao, et al., "Surface oxidation of palladium nanocrystals," Nanoscale, vol. 9, pp. 6327–6333, 2017.
[29] R. Sharma, A. Dhillon, and D. Kumar, "Colorimetric detection of Al (III) with silver nanoparticles," Sci. Rep., vol. 8, p. 5189, 2018.
[30] R. Dash and A. S. Bhattacharyya, "Ni-doped CuO nanocrystallites growth mechanism," MRS Adv., vol. 8, pp. 937–942, 2023.
[31] R. López González, M. H. Gutiérrez, R. L. García, S. A. Gómez Cornelio, C. Lobato, A. Gómez-Rivera, et al., "ZnO nanomaterials via Eichhornia crassipes," J. Chem. Technol. Biotechnol., vol. 99, pp. 2535–2544, 2024.
[32] M. Alavi, S. Dehestaniathar, S. Mohammadi, A. Maleki, and N. Karimi, "Phytofabricated ZnO and CuO NPs antibacterial activity," Adv. Pharm. Bull., vol. 11, pp. 497–505, 2020.
[33] O. Taylan, N. Cebi, and O. Sagdic, "ATR-FTIR spectroscopy of Mentha oils," Foods, vol. 10, p. 202, 2021.
[34] V. V. Makarov, A. J. Love, O. V. Sinitsyna, S. S. Makarova, I. V. Yaminsky, M. E. Taliansky, et al., "Synthesis of metal nanoparticles using plants," Acta Naturae, vol. 6, pp. 35–44, 2014.